https://doi.org/10.5194/acp-2020-501
Preprint. Discussion started: 21 July 2020

Atmospheric Chemistry and Physics Discussions

Fine particle pH and sensitivity to NH_3 and HNO_3 over summertime South Korea during KORUS-AQ

Ifayoyinsola Ibikunle[1], Andreas Beyersdorf[2], Pedro Campuzano-Jost[3,4], Chelsea Corr[2+], John D. Crounse[5], Jack Dibb[6], Glenn Diskin[7], Greg Huey[8], Jose-Luis Jimenez[3,4], Michelle J. Kim[5], Benjamin A. Nault[3,4], Eric Scheuer[6] Alex Teng[5], Paul O. Wennberg[5], Bruce Anderson[2], James Crawford[2], Rodney Weber[*8], Athanasios Nenes[*8,9,10]

[1]School of Chemical and Biomolecular Engineering, Georgia Institute of Technology, Atlanta, GA 30332, USA
[2]NASA Langley Research Center, Hampton, VA 23681, USA
[3]Department of Chemistry, University of Colorado, Boulder, CO 80309, USA
[4]Cooperative Institute for Research in Environmental Sciences, University of Colorado, Boulder, CO 80309, USA
[5]California Institute of Technology, Pasadena, CA 91125
[6]Institute for the Study of Earth, Oceans, and Space, University of New Hampshire, Durham, NH 03824, USA
[7]NASA Ames Research Center, Moffett Field, CA 94035, USA
[8]School of Earth and Atmospheric Sciences, Georgia Institute of Technology, Atlanta, GA 30332, USA
[9]School of Architecture, Civil & Environmental Engineering, Ecole Polytechnique Fédérale de Lausanne, CH-1015, Lausanne, Switzerland
[10]Center for the Study of Air Quality and Climate Change, Institute for Chemical Engineering Sciences, Foundation for Research and Technology Hellas, Patras, GR-26504, Greece
[+]Currently at Colorado State University

*correspondence to athanasios.nenes@epfl.ch and rweber@eas.gatech.edu

https://doi.org/10.5194/acp-2020-501
Preprint. Discussion started: 21 July 2020

Atmospheric Chemistry and Physics Discussions

Abstract

Using a new approach that constrains thermodynamic modeling of aerosol composition with measured gas-to-particle partitioning of inorganic nitrate, we estimate the acidity levels for aerosol sampled in the South Korean planetary boundary layer during the NASA/NIER KORUS-AQ field campaign. The pH (mean ± 1σ = 2.43±0.68) and aerosol liquid water content determined were then used to determine the "chemical regime" of the inorganic fraction of particulate matter (PM) sensitivity to ammonia and nitrate availability. We found that the aerosol formation is always sensitive to HNO_3 levels, especially in highly polluted regions, while it is only exclusively sensitive to NH_3 in some rural/remote regions. Nitrate levels are further promoted because dry deposition velocity is low and allows its accumulation in the boundary layer. Because of this, HNO_3 reductions achieved by NO_x controls prove to be the most effective approach for all conditions examined, and that NH_3 emissions can only partially affect PM reduction for the specific season and region. Despite the benefits of controlling PM formation to reduce ammonium-nitrate aerosol and PM mass, changes in the acidity domain can significantly affect other processes and sources of aerosol toxicity (such as e.g., solubilization of Fe, Cu and other metals) as well as the deposition patterns of these trace species and reactive nitrate.

1. Introduction

Poor air quality from high concentrations of fine particulate matter over South Korea has its origin in domestic emissions from vehicles, industry, and biomass burning, combined with long-range transport of pollutants from mainland China (Kim et al., 2018; Nault et al., 2018). Because air quality in South Korea is a mixture of factors such as regional and local emissions from both anthropogenic and natural (e.g. dust) sources, as well as meteorological (e.g. wind, relative

https://doi.org/10.5194/acp-2020-501
Preprint. Discussion started: 21 July 2020


Atmospheric Chemistry and Physics Discussions

humidity) and chemical interactions (e.g. photochemistry), assessing possible air pollution control strategies in this region is challenging (RSSR, 2016).

To improve our understanding of poor air quality in South Korea, the Korean National Institute of Environmental Research (NIER) and the United States National Aeronautics and Space Administration (NASA), conducted a field study in South Korea from 26 April to 18 June 2016 (RSSR, 2016). The aim of the Korea-United States Air Quality Study (KORUS-AQ), was to determine the factors that contribute to the poor regional air quality to aid the development of effective air quality mitigation strategies.

During the KORUS-AQ campaign, secondary production of particulate matter (PM) – organic and inorganic – constitute a significant fraction of PM pollution, with significant contribution from local sources. Since sulfate and nitrate comprised nearly half of the mass of PM at sizes smaller than 1um (PM_1) (Jordan et al., in review; Nault et al., 2018), aerosol acidity, liquid water content and temperature will significantly affect aerosol properties including its mass through the gas-particle partitioning of semi-volatile species (Nenes et al., 2020a). More broadly, fine aerosol particle acidity in South Korea affects air quality and human health and therefore requires knowledge of aerosol pH levels (e.g., Nenes et al., 2020a).

Given that direct measurement of atmospheric aerosol pH remains a challenge, there is large uncertainty in this important parameter (Pye et al., 2020). Of all approaches used to date for constraining aerosol pH, use of thermodynamic analysis of gas-aerosol observations together with a model provides the most robust estimates of aerosol acidity (Hennigan et al., 2015; Song et al., 2018; Pye et al., 2020). To achieve the most robust pH predictions, thermodynamic analysis requires observations of all species, both gas and particle phase, that affect pH. Knowledge of gas-phase ammonia and particulate ammonium is especially important, owing to its role as the

https://doi.org/10.5194/acp-2020-501
Preprint. Discussion started: 21 July 2020


Atmospheric Chemistry and Physics Discussions

dominant cation in fine-mode aerosol and pH-sensitive partitioning. Accurate measurement of ammonia, especially at low concentrations, is far from trivial (Zhu et al., 2015; Wang et al., 2015) and subject to biases from adsorption of NH_3 in instrument inlets and NH_4^+ volatilization (Dawson et al., 2014; Osada 2011; Yokelson et al., 2003; Guo et al., 2018a). Although measurements of aerosol NH_4^+ are common, gas-phase measurements of NH_3 are often missing in field studies – including for KORUS-AQ. There is a need to accurately infer aerosol pH in the absence of gas-phase NH_3 data.

This study aims to accurately determine fine particle pH for aerosol in South Korea, and use this inferred pH to understand the sensitivity of PM mass to the availability of ammonia and nitric acid (which are two major aerosol precursors). Focusing only on the inorganic fraction of the aerosol, we develop a computationally rigorous approach to estimate aerosol pH and particle liquid water despite missing gas-phase ammonia data and apply it to the KORUS-AQ dataset. We then utilize these data to assess optimal strategies to control inorganic aerosol mass through reduction of either available nitric acid or ammonia, based on the new approach of Nenes et al. (2020a).

2. Methods

2.1 Instrumentation

Non-refractory PM_1 composition

The CU-Boulder highly-customized Aerodyne high-resolution time-of-flight aerosol mass spectrometer (HR-ToF-AMS) measured non-refractory (NR) PM_1 composition, including ammonium, nitrate, sulfate, chloride, and organic aerosol. The basic concept, operation, and aircraft deployment of the AMS has been described elsewhere (DeCarlo et al., 2006, 2008; Dunlea et al., 2009; Kimmel et al., 2011) and the deployment for KORUS-AQ is discussed in detail by

https://doi.org/10.5194/acp-2020-501
Preprint. Discussion started: 21 July 2020


Atmospheric Chemistry and Physics Discussions

Nault et al. (2018). Observations are reported in units of μg sm^{-3} (under standard conditions of T=273.15 K, p=1013 hPa). For the following analysis, the data were converted to concentrations at ambient conditions for the thermodynamic calculations.

The AMS also separately measures the contribution of amines, organonitrates and organosulfates (Fry et al., 2019; Farmer et al., 2010; Chen et al., 2019). During the campaign, organic nitrates comprised roughly 8% of the AMS particulate NO_3 signal and were only an important contribution to the signal when NO_3 was below 0.50 μg sm^{-3} (0.45 μg m^{-3}) (Nault et al., 2018). Average concentration of nitrate during the campaign was 8.09 ± 6.16 μg m^{-3}, so we consider AMS nitrate to be approximately equal to inorganic aerosol NO_3^-. Accuracy (2σ) for AMS detection of inorganic species is estimated to be 35% (Bahreini et al, 2009).

Gas-phase HCl and HNO_3

HCl and HNO_3 measurements were made using the Georgia Institute of Technology Chemical Ionization Mass Spectrometer (GT CIMS) and the California Institute of Technology CIMS (CIT CIMS), respectively. The GT CIMS technique utilizes a low-pressure ion source/reactor and SF_6^- reagent ion chemistry to detect HCl (Huey et al., 2004; Slusher et al., 2004, Kim et al., 2007). The CIT CIMS utilizes CF_3O^- chemistry to detect HNO_3 by way of fluoride transfer (Huey et al., 1996; Amelynck et al., 2000; Crounse et al., 2006). Both methods are configured to allow for ion chemistry in a heated Teflon-coated flow tube at low pressure to selectively cluster the reagent ions with HNO_3 (HCl) in ambient air (Huey et al., 2004). The ions from the flow tube enter a mass spectrometer, where they are mass-analyzed and quantified. Gas-phase concentrations were reported in ppbv (parts-per-billion, by volume), and were subsequently converted to μg m^{-3} at ambient conditions prior to thermodynamic analysis. The estimated CIMS measurement uncertainty is 40%.

https://doi.org/10.5194/acp-2020-501
Preprint. Discussion started: 21 July 2020


Atmospheric Chemistry and Physics Discussions

120

121 *Non-volatile aerosol cations and meteorological variables*

122 Non-volatile cations, such as Na^+, K^+, Ca^{2+}, and Mg^{2+}, were measured using the soluble acidic
123 gases and aerosols (SAGA) instrumentation. Bulk aerosol (nominally < 4.1 μm aerodynamic
124 diameter) are collected onto filters to quantify soluble ions (Dibb et al., 2003). Detection limits are
125 5 pptv for Mg^{2+} and better than 20 pptv for Na^+, K^+, and Ca^{2+}
126 (https://cloud1.arc.nasa.gov/docs/intex-b/SAGA_Dibb.pdf). Filter sampling times were
127 approximately 5 min or less. Units of NVCs were reported in μg m^{-3} under ambient conditions
128 when used for thermodynamic calculations. Water vapor content was measured using a diode laser
129 hygrometer (Diskin et al., 2002) and then converted to relative humidity based on the measurement
130 of temperature measured onboard.

131

132 **2.2 Thermodynamic analysis of observations and PM sensitivity to aerosol precursors**

133 ISORROPIA II (Fountoukis and Nenes, 2007; http://isorropia.epfl.ch), was used to calculate the
134 equilibrium phase state and composition of inorganic aerosol systems containing NH_4^+ , SO_4^{2-},
135 NO_3^-, Cl^-, Na^+, Ca^{2+}, K^+, Mg^{2+}, aerosol liquid water content, and partitioning of semi-volatile
136 species (e.g. particle nitrate, NO_3^-, and gas phase nitric acid, HNO_3). ISORROPIA was run in
137 forward mode, which results in more robust and accurate predictions of pH owing to the sensitivity
138 of reverse mode calculations to measurement uncertainty (Hennigan et al., 2015; Song et al., 2018).
139 The model assumes that fine particles and their corresponding volatile counterparts are in
140 thermodynamic equilibrium, which is a good assumption for submicron particles that are not
141 kinetically limited by size (i.e., in the fine mode) (Dassios and Pandis 1999; Cruz and Pandis 2000;
142 Fountoukis et al., 2009) and slow diffusivity in the particle phase. For the selected KORUS-AQ

https://doi.org/10.5194/acp-2020-501
Preprint. Discussion started: 21 July 2020


Atmospheric Chemistry and Physics Discussions

143 dataset (<1 km ASL, 45% < RH < 95%, average RH: 62±12%; average temperature: 20.2±2.5 C)
144 the aerosol tends to be in a liquid metastable state (i.e. no precipitation of salts under supersaturated
145 conditions; Fountoukis and Nenes 2007; Day and Malm 2001; Seinfeld and Pandis, 2016).
146 Efflorescence typically occurs for RH between 10-30%, however, such humidity points were not
147 considered in our analysis.

148 While ISORROPIA II can handle systems containing non-volatile cations (NVCs), such as Na^+,
149 K^+, Mg^{2+}, and Ca^{2+}, they were not considered in the analysis owing to their very low concentration
150 (Figure 1) and minor impact on aerosol pH (Guo et al., 2018a); as well as, the fact that much of
151 the NVCs were in the supermicron mode (Saide et al., 2019; Heim et al., 2020). A sensitivity
152 calculation, using SAGA measurements as an upper limit of submicron NVCs pH confirms this
153 (Table 1).

154 ISORROPIA II is used to calculate the pH of aerosols. pH is defined as:

155 $$pH = -log_{10}(\gamma_{H^+} H^+_{aq}) = -log_{10}(\frac{1000\,\gamma_{H^+}\,H^+_{air}}{W_i + W_o}) \approx -log_{10}(\frac{1000\,\gamma_{H^+}\,H^+_{air}}{W_i}) \quad (1)$$

156 where $\gamma_{H+}$is the hydronium ion activity coefficient – here assumed to be unity, H^+_{aq} (mol L^{-1})
157 hydronium ion concentration in aerosol liquid water, H^+_{air} (µg m^{-3}) hydronium ion concentration
158 per volume of air, and W_i (µg m^{-3}) and W_o (µg m^{-3}) are the particle liquid water concentrations
159 associated with inorganic and organic species, respectively. Although W_o can be estimated, e.g.,
160 through the hygroscopicity parameter (e.g., Guo et al., 2015), its effect on pH, together with
161 organic effects on the activity coefficient, are secondary - introducing somewhere between a 0.15
162 and 0.30 pH units change (Guo et al., 2015; Song et al., 2018; Vasilakos et al., 2018; Battaglia Jr.
163 et al., 2019). Note Equation 1 is consistent with the "pH_F" definition of Pye et al. (2020).

https://doi.org/10.5194/acp-2020-501
Preprint. Discussion started: 21 July 2020


Atmospheric Chemistry and Physics Discussions

As applied here, the thermodynamic analysis provides pH consistent with "bulk" pH, which assumes that particles are internally mixed. This assumption tends to provide good estimates of pH for submicron particles, given that the equilibrium assumption is largely satisfied and semi-volatile partitioning of gases such as NH_3 and HNO_3 is well captured (Guo et al., 2018b, Pye et al., 2020). Internal mixing is achieved in a few hours in polluted areas due to rapid secondary aerosol production (Wang et al., 2010; Zhu et al., 2016; Riemer et al., 2019). Both the ground AMS (Kim et al., 2018) and the aircraft AMS (Nault et al., 2018) saw no evidence of external mixing based on the mass size distributions of the individual components, so the internal mixing assumption is appropriate.

The results of the thermodynamic analysis are then combined with the conceptual framework of Nenes et al. (2020a) to identify the chemical domains of PM mass sensitivity to HNO_3 and NH_3 availability for this observational dataset. These sensitivity domains are characterized as *i*) primarily NH_3-sensitive, *ii*) primarily HNO_3-sensitive, *iii*) combined NH_3 and HNO_3 sensitive, and, *iv*) HNO_3/ NH_3 insensitive. This thermodynamically consistent approach enables us to directly determine how change in gas phase species will elicit a change in PM mass. As it pertains to the KORUS-AQ campaign, we adopt the Nenes et al. (2020a) threshold value for nitrate and ammonia partitioning that separates each regime at the 10% level. For example, for nitrate this means that when more than 10% of the total nitrate is in the particle phase, we would expect PM responses to NO_3^- precursors to be significant.

2.4 Nitrate partitioning constrained pH (NPC-pH)

When the thermodynamic model is run in forward mode, input of semi-volatile species (i.e., those that can exist in particle- or gas-phase) are assumed to be total gas and particle concentrations. As

https://doi.org/10.5194/acp-2020-501
Preprint. Discussion started: 21 July 2020


Atmospheric Chemistry and Physics Discussions

187 in this study, when NH_3 data is unavailable, the total NH_3 will be lower than the true value, as
188 some fraction of the total NH_3 is actually in the gas phase. In these cases, particle acidity is likely
189 to be overestimated. Past studies have proposed an iterative approach to calculate pH and gas phase
190 ammonia data (e.g., Guo et al., 2016) that involves running ISORROPIA (without gas-phase
191 ammonia) to retrieve the predicted equilibrium gas phase ammonia concentration from the model
192 output. This equilibrium NH_3 along with the measured NH_4^+ is then used as total ammonia input
193 for the next ISORROPIA iteration (which eventually adds some mass to the system), holding all
194 other input values constant. After each such iteration, convergence is checked by examining
195 whether the values of gas-phase NH_3 agree to within a predefined criterion. This method, however,
196 is unconditionally unstable, i.e., the method does not converge when an increasingly strict criterion
197 is used (see Figure 2 for a schematic). To demonstrate this, Figure 3 presents how pH and gas-
198 phase NH_3 change with iteration; a stable algorithm would eventually converge to values that do
199 not change with iteration; in reality NH_3 and pH increase monotonically without a bound. This
200 instability is not unique to ISORROPIA, but inherent to the algorithm and should apply to any
201 thermodynamic model, as the amount of total ammonia with every iteration increases – without
202 any bound. Applying a less strict upper bound would result in an arbitrary estimate of total
203 ammonia, which requires some prior knowledge on NH_3 levels to provide realistic values of pH
204 (which is what Guo et al., 2016 adopted).

205 As an alternative to the Guo et al. (2016) algorithm, we propose a method to infer pH calculations
206 from thermodynamic analysis of observations when NH_3 data are lacking. This approach involves
207 using an algorithm that is tied to the observed nitrate/nitric acid partitioning (hereafter referred to
208 as "nitrate partitioning constrained pH", NPC-pH) to infer gas-phase NH_3 concentrations required
209 for plausible pH predictions. Figure 4 summarizes the methodology behind this approach. The

https://doi.org/10.5194/acp-2020-501
Preprint. Discussion started: 21 July 2020


Atmospheric Chemistry and Physics Discussions

observed NH_4^+, total nitrate, and nitrate partitioning fraction, $\varepsilon(NO_3)$—defined as the fraction of total nitrate (gas + aerosol) present in the aerosol phase—are used as input to an iterative algorithm that determines the value of gas-phase NH_3 that, together with the observed value of NH_4^+, temperature, and relative humidity reproduces the observed $\varepsilon(NO_3)$ to some predetermined level of accuracy. The thermodynamic calculations required for each step in the iterative procedure are done with ISORROPIA-II. Upon convergence (here, to within 10^{-6} between iterations), particle liquid water, H^+_{air} concentration, and particle pH are obtained and used for further analysis. In the following, we assess the predicted pH with NPC-pH, which together with aerosol liquid water content is needed to determine an effective PM control strategy.

Nitric acid can condense onto fine mode and coarse particles containing non-volatile cations (from seasalt or dust). Because of this, nitrate may over time volatilize and recondense onto coarse mode cations forming nonvolatile species (in the form of $Ca(NO_3)_2$, $NaNO_3$ and other salts). This disequilibrium will lead to a gas phase HNO_3 concentration which is lower than the equilibrium value expected from the PM_1 composition and higher than the corresponding value based on the coarse mode composition. Given that the equilibration timescale of submicron aerosol is much smaller than for coarse mode particles, the degree of disequilibrium between the PM_1 nitrate and gas-phase HNO_3 is much smaller than that for coarse mode nitrate. We therefore assume that the PM_1 semi-volatile inorganic species (NO_3^-, NH_4^+) are in equilibrium with their gas phase components (HNO_3, NH_3). Analysis carried out by Guo et al. (2017) supports this approach.

2.5 Data selection and analysis

Data points were filtered for conditions where ambient relative humidity (RH) fell within the range of 45-95%, and flight altitude below 1 km which is often within the boundary layer and most

https://doi.org/10.5194/acp-2020-501
Preprint. Discussion started: 21 July 2020


Atmospheric Chemistry and Physics Discussions

relevant from an air quality perspective (the sampling RH was often significantly lower, but exposure to these low levels of humidity is too short to have a significant impact on semi-volatile nitrate and ammonium; Shingler et al, 2016; Guo et al., 2017). The RH range was chosen to ensure robust estimations from the thermodynamic model. Data for RH > 95% were excluded owing to the exponential growth in particle liquid water with RH, which leads to high W_i and subsequently large pH uncertainty owing to propagation of RH uncertainties (Guo et al., 2015). Guo et al. (2016) suggests that below RH of 40%, pH estimations are subject to considerable uncertainty owing to the low aerosol liquid water and other uncertainties, which limits the ability to capture the observed partitioning of nitrate and other species. From this filtering process, a total of 11 of the total flights were analyzed and are summarized in Table S1.

3. Results

3.1 Sensitivity studies to evaluate the new NPC-pH algorithm

The NPC-pH algorithm for predicting pH without NH_3 data was assessed based on a synthetic dataset for which aerosol is in perfect thermodynamic equilibrium. To this dataset, random variability is added to the concentration of semi-volatile species (within a predefined but relatively wide range). The NPC-pH algorithm was applied to the original and noisy synthetic data sets, to predict pH. The aerosol acidity obtained from NPC-pH was then compared to the pH of the initial data where the aerosol was in equilibrium with all species. The robustness of the acidity to noise level is important, especially given that aerosol semivolatile species could be in disequilibrium.

The synthetic data was constructed of aerosol precursor values relevant for KORUS-AQ conditions: total NO_3 concentration ranged from 0.2 to 110 μg m^{-3} allowing for $\varepsilon(NO_3)$ to range

https://doi.org/10.5194/acp-2020-501
Preprint. Discussion started: 21 July 2020

Atmospheric Chemistry and Physics Discussions

from 0-0.95. Total SO_4 and total NH_4^+ concentrations ranged from 0.1-10 µg m^{-3} and 0.2-110 µg m^{-3}, respectively. $\varepsilon(NH_4)$ ranged from 0-1. The total Cl concentration was kept constant at 0.50 µg m^{-3} and NVC concentrations were set to zero. Temperature was kept constant at 298K, and the RH ranged from 45-95%. Comparing the equilibrium partitioning retrieved from the synthetic data (without added noise) to that generated from the algorithm resulted in nearly perfect agreement between the two quantities, when $\varepsilon(NO_3)$ was greater than about 40% (Figure 5). Higher sensitivity of low $\varepsilon(NO_3)$ values to pH and gas-phase NH_3 results in more scatter in $\varepsilon(NO_3)$ generated from the algorithm for $\varepsilon(NO_3) < 0.4$. Average pH for the whole synthetic dataset for equilibrium and NPC-pH method are 2.14 ± 1.33 and 2.26 ± 1.25, respectively while the average LWC for equilibrium and NPC-pH method are 42.50 ± 137.85µg m^{-3} and 42.25 ± 137.93 µg m^{-3}, respectively. The large standard deviation is a result of a wide range of conditions tested during the analysis.

To ascertain how uncertainties in nitrate partitioning (i.e., deviations from thermodynamic equilibrium) would impact pH inferences from NPC-pH, random noise at the 1-50% level is added to the original $\varepsilon(NO_3)$ values from the synthetic dataset. Reapplication of NPC-pH to the noisy datasets then quantify the effect of this noise to the inferred pH. The method used to add noise is shown in equations 2 and 3

$$X = 2\Phi\left(-\frac{1}{2} + Rnd\right)\varepsilon(NO_3) \quad (2)$$

$$\varepsilon(NO_3)_{Rnd} = \varepsilon(NO_3) + X \quad (3)$$

where $\varepsilon(NO_3)_{Rnd}$ is $\varepsilon(NO_3)$ with added random noise X that is symmetrical about zero and scaled to the magnitude of $\varepsilon(NO_3)$; Φ is the maximum fractional noise level (ranging from 0.01-0.5 to express a noise level of 1-50%) and *Rnd* is a random number between 0 and 1, generated by the "`rand()`" pseudorandom number generator available in the Matlab® environment.

https://doi.org/10.5194/acp-2020-501
Preprint. Discussion started: 21 July 2020


Atmospheric Chemistry and Physics Discussions

Results from this sensitivity analysis reveal that a 50% relative error in $\varepsilon(NO_3)$ resulted in an average absolute error in pH of 0.28±0.45 units, and explained as follows. Figure 6 presents $\varepsilon(NO_3)$, $\varepsilon(NH_4)$ and pH for T= 288 K, and with average ISORROPIA-predicted liquid water content (13.78±10.52 μg m^{-3}) and activity coefficients (0.125 and 1.794 for $\gamma_{NO3-}\gamma_{H+}$ and $\gamma_{H+}/\gamma_{NH4+}$, respectively) derived from the KORUS-AQ flight data analysis (Table 1). In the blue region, where $\varepsilon(NO_3)$ approaches 0 or 1, we observe that a small uncertainty in $\varepsilon(NO_3)$ can result in significant changes to pH. In the pink region, however, we would expect that even large changes in $\varepsilon(NO_3)$ would only result in minor changes to pH. Evaluating 0.2< $\varepsilon(NO_3)$ <0.8 from the synthetic data resulted in an average absolute error in pH of 0.21±0.15 units. Therefore, pH predictions using this method are reasonably accurate, especially when considering the inherent uncertainty of pH inferences using thermodynamic models (Pye et al. 2020) and the low sensitivity of pH to NH_3 inferences error (about a factor of 10 error in NH_3 provides a pH error of 1 unit, regardless of acidity regime; Guo et al., 2017; Song et al., 2019).

3.2 Aerosol acidity during KORUS-AQ

KORUS-AQ integrated aircraft and ground-based measurements, and satellite observations. The campaign was conducted over South Korea (33 and 39 ^{o}N, 124 and 130E ^{o}E) and the Yellow Sea during the months of May and June in 2016. Flight tracks for the DC-8 during KORUS-AQ are shown in Figure 7, colored by measured concentrations of NO_3^-. Most flights focused on the western region (35 and 38 ^{o}N, 126 and 127^{o}E) of South Korea extending into the Yellow Sea. Major emitters of NO_x are the Taean coal power plant (36.90 °N, 126.23 °E), Dangjin power plant (37.06°N, 126.51°E), and Yeongheung power station (37.24°N, 126.44°E) – which are all within the region of observed high nitrate concentrations (Hong et al. 2019; Kafle et al. 2017; Kim et al.

https://doi.org/10.5194/acp-2020-501
Preprint. Discussion started: 21 July 2020


Atmospheric Chemistry and Physics Discussions

2013). Increased nitrate levels observed in Table 1 for Asia are most likely the result of emissions from vehicular traffic and power plants, and active photochemistry (Nault et al., 2018) and nighttime nitrate formation from N_2O_5 hydrolysis (Jordan et al., 2019). More details on KORUS-AQ flights can be found in Nault et al. (2018).

Measurements of HNO_3 and NO_3^- indicate that $\varepsilon(NO_3)$ most of the time (approximately 92%; Figure S3) falls between 0.1 and 0.9, indicating that aerosol nitrate levels will be sensitive to pH (i.e., reside in the "sensitivity window" of Vasilakos et al., 2018; Figure 6). Of the remaining 8%, approximately 6% of these partitioning values fall below 0.1, while 2% of all nitrate partitioning measurements were greater than 0.9, where nitrate partitioning is expected to be less sensitive to pH changes. Given this and the sensitivity analysis of Section 3.1, the NPC-pH algorithm can provide robust estimates of aerosol pH for the majority of the KORUS-AQ data. We find that the average pH for all flights was 2.43±0.68 (Table 1), while the average acidity between flights varied between 1.74 and 2.90 (Table S1). These pH levels are similar to what has been reported by others in the region for summertime conditions; Spring in Beijing, China (pH range= 1.8-4.3) (Ding et al., 2019; Tan et al., 2018; Wang et al., 2019; Pye et al. 2020).

The inorganic fraction of the KORUS-AQ aerosol is dominated by sulfate, ammonium, and nitrate (Figure 1). Since as already mentioned in the methods the relative mass concentrations of NVCs to other major inorganic ion components are low, we assume the formation of nonvolatile salts (e.g. $Ca(NO_3)_2$ and $Na(NO_3)$) negligibly impact the pH derived from nitrate partitioning. This assumption is valid as the pH calculated using SAGA measurements of NVCs is within 1% of that predicted, consistent with the impact suggested by Guo et al. (2018a). We also do not consider the contribution of organic nitrates to the total amount of nitrates (which constitute less than 10% of

https://doi.org/10.5194/acp-2020-501
Preprint. Discussion started: 21 July 2020


Atmospheric Chemistry and Physics Discussions

the total nitrate, hence have a minimal impact on liquid water content and pH, based on the analysis in Section 3.1).

Particle pH is affected by several coupled variables such as particle nitrate and nitrate partitioning levels. Higher ambient particle pH is often associated with higher concentrations of particle nitrate (Guo et al., 2018b). This occurs when nitrate aerosol (usually in the form of ammonium nitrate) dominates the aerosol liquid water content; in such situations, the aerosol can contain considerable amounts of aerosol water but maintain small amounts of H^+ in solution – as it tends to combine with NO_3^- to form volatile HNO_3. In contrast, when aerosol liquid water is controlled by hygroscopic sulfates, significant amounts of H^+ can exist in solution (e.g., from the semi-volatile partitioning of NH_4^+ to form NH_3) as its tendency to associate with HSO_4^-, SO_4^{-2} is relatively weak and sulfates are involatile. This general effect of higher (lower) pH associated with higher (lower) NO_3 has been seen in a number of other field campaigns (see comparisons in Table 1). In Cabauw, Netherlands during the summer, Guo et al. (2018b) reported an $\varepsilon(NO_3)$ of 88%, with a corresponding pH of 3.3±0.5. Both quantities are higher than the values found for the KORUS-AQ campaign. The pH of aerosol in Beijing, China in the summer was found to be 3.9±1.3 for nitrate levels that are higher than those measured for the South Korean data (Table 1).

3.3 Acidity and PM sensitivity regimes to NH_3 and HNO_3 during KORUS-AQ

Nenes et al. (2020a) developed a framework that allows PM sensitivity to NH_3 and HNO_3 availability to be determined from aerosol acidity and liquid water content. This framework directly determines effective PM reduction policies – which is important given recent work identifying NH_3 reductions over other policies (e.g., NO_x and SO_x reductions) (Pozzer et al., 2017;

https://doi.org/10.5194/acp-2020-501
Preprint. Discussion started: 21 July 2020


Atmospheric Chemistry and Physics Discussions

345 Xu et al., 2019) as the most effective for PM reductions, and the dominance of PM in the region
346 by ammonium and nitrate (22.2 and 36.6%, respectively; Figure 1)
347 In its simplest form, the Nenes et al. (2020a) framework is expressed in terms of a "policy map"
348 (Figure 8) characterized by four distinct regimes: one, shaded pink, where $\varepsilon(NO_3)$ is small and
349 $\varepsilon(NH_4)$ is large (i.e., the majority of nitrate resides in the gaseous phase and ammonia in the particle
350 phase, defined by a relevant threshold); here PM mass responds proportionally to changes in the
351 total ammonia but tends to be insensitive to total nitrate changes. For this reason, Nenes et al.
352 (2020a) characterize PM in this regime as being "NH_3 sensitive". The opposite is seen in the blue-
353 shaded regime, as the majority of nitrate resides in the aerosol phase and ammonia in the gas phase.
354 For this reason, Nenes et al. (2020a) characterize PM in this region as being "HNO_3 sensitive". In
355 both acidity regimes, partitioning may not be strongly affected by pH changes, therefore
356 uncertainties in its exact value carry minor implications for PM sensitivity to available ammonia
357 and nitrate. In the purple acidity domain, however, which Vasilakos et al. (2018) terms "sensitivity
358 window", PM tends to respond to both HNO_3 and NH_3 emissions, as an important fraction of both
359 species is in the aerosol phase (Nenes et al., 2020a). Here, rather precise knowledge of aerosol pH
360 is important – as variations to within one unit usually imply a very large change in the partitioning
361 fraction for each semi-volatile species, hence PM sensitivity. The fourth domain, colored white, is
362 characterized by low nitrate and ammonium partitioning fraction, and PM is then relatively
363 insensitive to changes in NH_3 and HNO_3 availability.
364 From the histogram of observed nitrate partitioning (Figure S3), we expect a large fraction of the
365 data to lie in the HNO_3/NH_3 sensitive domain. As distribution of nitrate partitioning is toward the
366 high end of $\varepsilon(NO_3)$ for the study (average nitrate partitioning value of 58±24%), PM_1 reductions
367 would be sensitive to reductions in HNO_3 – hence NO_x reductions. Indeed, if the pH and aerosol

https://doi.org/10.5194/acp-2020-501
Preprint. Discussion started: 21 July 2020


Atmospheric Chemistry and Physics Discussions

liquid water content for the KORUS-AQ data are plotted on the policy map (Figure 8), the data reside in the domain where HNO_3 or a mix of HNO_3/NH_3 controls are generally the most effective routes for reduction of inorganic PM_1 mass for the time period of the study.

Focusing on flights that span the nitrate $\varepsilon(NO_3)$ range with high HNO_3 availability provides additional insights on effective PM controls: during flight 19 the highest levels of nitrate and ammonium of the mission were measured; and in contrast during flight 15 approximately 30% of its ambient nitrate partitioning values fell below 0.1 (Figure S4; other per-flight characteristics can be found in table S1). High levels of nitrate availability are expected for flight 19 because of its proximity to a number of power plants (and associated NO_x emissions) along the northwest coast. The DC-8 aircraft also flew very close to Seoul, South Korea for this flight (see Figure S1) – an area where nitrate availability from vehicular NO_x emissions are expected to be large. Plotting the data from both flights on the Nenes et al. (2020a) policy map indicates where the high HNO_3 availability can lead to high NO_3^- levels. The results (Figure 9) suggest that data from each flight reside mostly in the NH_3-HNO_3 sensitivity domain, which implies similar emissions control strategies are effective, despite the very different aerosol characteristics in both flights.

The above analysis can be further expanded to consider only PM levels above a regulatory mass threshold, as PM control policies are most effective when relevant for the high PM levels seen in pollution events. To assess this, we plot all the available data on the policy map, but with points color-coded with PM level (Figure 10). For PM levels exceeding e.g., 30 $\mu g\ m^{-3}$, HNO_3 is always an effective control strategy, while NH_3 is effective for about half the points. The relatively fewer cases that fall into the NH_3-sensitive domain are characterized by low PM levels, hence less important to control. Given that dry deposition dominates the loss of boundary layer PM during haze episodes, and the expected low deposition rate of nitrate when $\varepsilon(NO_3)$ is relatively large

https://doi.org/10.5194/acp-2020-501
Preprint. Discussion started: 21 July 2020


Atmospheric Chemistry and Physics Discussions

(Nenes et al., 2020b) further emphasizes the need to control NO_x, as such conditions favor the rapid accumulation of available HNO_3 – and buildup of the high levels of NO_3^-seen in the observations (Figure 1).

4. Summary and broader implications

Accurate estimates of atmospheric aerosol acidity are important for understanding a number of atmospheric processes sensitive to pH. Here, we present a method – called NPC-pH - for estimating aerosol pH, through thermodynamic analysis of observations that lack gas-phase ammonia measurements. NPC-pH is based on the observed gas-to-particle partitioning of nitrate in the absence of ammonia measurements, and is shown to perform much better than a previously proposed algorithm that iterated for total ammonia (using aerosol ammonium as an initial guess), as the latter is shown to be unconditionally unstable. NPC-pH is also shown to provide robust pH levels that are relatively insensitive to nitrate partitioning errors.

Applying NPC-pH to airborne observations collected from the NASA/NIER KORUS-AQ field campaign in South Korea resulted in pH predictions (pH=2.43 ± 0.68) that are consistent with published estimates in this region and season. The pH and LWC calculated from our thermodynamic analysis and the approaches of Nenes et al. (2020ab) determine the "chemical regime" of PM sensitivity to ammonia and nitrate availability, and, "dry deposition velocity regime" of inorganic nitrogen (which controls the lifetime, hence accumulation, of nitrate in the boundary layer during haze episodes). For KORUS-AQ, we found that the aerosol formation is often in the NH_3 and HNO_3-sensitive or HNO_3-sensitive zone, while a small fraction (4%) of the points fall in NH_3-limited region near the Yellow Sea, Jeju Island, Busan and Eastern Sea. Nevertheless, when PM levels are high, the data always lies in the HNO-sensitive or HNO_3/NH_3 – sensitive region. Under these conditions, we conclude that HNO_3 reductions prove to be the most

https://doi.org/10.5194/acp-2020-501
Preprint. Discussion started: 21 July 2020


Atmospheric Chemistry and Physics Discussions

414 effective for all conditions examined, and that NH_3 emissions would only partially be effective in
415 reducing PM levels – especially given that during pollution episodes, the pH and LWC levels
416 promote rapid accumulation of nitrate aerosol in the boundary layer owing to its slow dry
417 deposition (Nenes et al., 2020b). A complete in-depth analysis of the complex chemistry and
418 contributions of different sources however is required to fully assess the most effective NO_x
419 emission controls to reduce HNO_3 production. Source attribution information can also be
420 represented on the policy maps shown here to understand their role in shaping the acidity, liquid
421 water, and PM sensitivity/deposition regimes (e.g., Zang et al., in review) to further refine types
422 of policies that could be effective during pollution episodes.
423 Despite the benefits of controlling PM formation to reduce ammonium-nitrate aerosol and PM
424 mass, we must consider that the acidity domain can significantly affect other processes and sources
425 of aerosol toxicity. Fang et al. (2017) and Wong et al. (2020) showed that acid-driven dissolution
426 of transition metals (e.g., Fe, Cu) can potentiate health effects such as cardiovascular morbidity
427 and mortality through oxidative stress (Bates et al., 2015; Ghio et al., 2012). If emissions controls,
428 in an attempt to reduce PM levels also lead to reduction in pH, may unintentionally increase aerosol
429 toxicity with adverse health effects in humans. Lastly, increased aerosol acidity can impact the
430 deposition pattern of reactive nitrogen (Nenes et al., 2020b) and bioavailability of micronutrients
431 (e.g. Fe, P) with both synergistic and/or antagonistic effects on remote ecosystems (e.g.,
432 Meskhidze et al., 2003; Nenes et al., 2011; Ito et al., 2016).
433

434 **Acknowledgements**

435 This work was supported by NASA grant NNX16AE19G (KORUS-AQ) and from PyroTRACH
436 (ERC-2016-COG) funded from H2020-EU.1.1. - Excellent Science - European Research Council

https://doi.org/10.5194/acp-2020-501
Preprint. Discussion started: 21 July 2020


Atmospheric Chemistry and Physics Discussions

437 (ERC), project ID 726165. JLJ, PCJ, and BAN (AMS) were supported by NASA grants
438 NNX15AT96G, 80NSSC19K0124, and 80NSSC18K0630. JDC, MKJ, AT, and POW (Caltech)
439 were supported by NASA grants NNX15AT97G.
440

441 **Author contributions**

442 II was responsible for the thermodynamic analysis of the ambient data, contributed to the ammonia
443 estimation algorithm and wrote the initial draft of the manuscript with significant contributions by
444 AN and RW. AN is a core developer of ISORROPIA-II, developed the conceptual framework used
445 here for understanding the sensitivity of PM2.5 to total nitrate and ammonia, the tools to include
446 the ambient data on the acidity maps and also demonstrated the unconditional instability of the
447 original NH_3 iteration algorithm of Guo et al. (2016). AN and RW were involved in planning and
448 supervision of the work. All authors provided feedback on the analysis approach and extensively
449 contributed to the manuscript text.
450

451 **Code and Data availability**

452 The ISORROPIA-II thermodynamic equilibrium code is available at http://isorropia.epfl.ch.
453 KORUS-AQ data is available at https://www-air.larc.nasa.gov/cgi-bin/ArcView/korusaq.
454

455 **Competing interests**

456 The authors declare that they have no conflicts of interest.

https://doi.org/10.5194/acp-2020-501
Preprint. Discussion started: 21 July 2020


Atmospheric Chemistry and Physics Discussions

References

Amelynck, C., N. Schoon, and E. Arijs. Gas phase reactions of CF3O− and CF3O−H2O with nitric, formic, and acetic acid, International Journal of Mass Spectrometry, 203: 165-75, 2000

Bahreini, R., B. Ervens, A. M. Middlebrook, C. Warneke, J. A. de Gouw, P. F. DeCarlo, J. L. Jimenez, C. A. Brock, J. A. Neuman, T. B. Ryerson, H. Stark, E. Atlas, J. Brioude, A. Fried, J. S. Holloway, J. Peischl, D. Richter, J. Walega, P. Weibring, A. G. Wollny, and F. C. Fehsenfeld. Organic aerosol formation in urban and industrial plumes near Houston and Dallas, Texas, Journal of Geophysical Research: Atmospheres, 114, 2009

Bates, Josephine T., Rodney J. Weber, Joseph Abrams, Vishal Verma, Ting Fang, Mitchel Klein, Matthew J. Strickland, Stefanie Ebelt Sarnat, Howard H. Chang, James A. Mulholland, Paige E. Tolbert, and Armistead G. Russell. Reactive Oxygen Species Generation Linked to Sources of Atmospheric Particulate Matter and Cardiorespiratory Effects, Environmental Science & Technology, 49: 13605-12, 2015

Chen, Y., Xu, L., Humphry, T., Hettiyadura, A. P. S. S., Ovadnevaite, J., Huang, S., Poulain, L., Schroder, J. C., Campuzano-Jost, P., Jimenez, J. L., Herrmann, H., O'Dowd, C., Stone, E. A., Ng, N. L., O'Dowd, C., Stone, E. A., Ng, N. L., O'Dowd, C., Stone, E. A. and Ng, N. L.: Response of the Aerodyne Aerosol Mass Spectrometer to Inorganic Sulfates and Organosulfur Compounds: Applications in Field and Laboratory Measurements, Environ. Sci. Technol., 53(9), 5176–5186, doi:10.1021/acs.est.9b00884, 2019

Crounse, John D., Karena A. McKinney, Alan J. Kwan, and Paul O. Wennberg. Measurement of Gas-Phase Hydroperoxides by Chemical Ionization Mass Spectrometry, Analytical Chemistry, 78: 6726-32, 2006

Cruz, Celia N., and Spyros N. Pandis. Deliquescence and Hygroscopic Growth of Mixed Inorganic−Organic Atmospheric Aerosol, Environmental Science & Technology, 34: 4313-19, 2000

Dassios, Konstandinos G., and Spyros N. Pandis. The mass accommodation coefficient of ammonium nitrate aerosol, Atmospheric Environment, 33: 2993-3003, 1999

https://doi.org/10.5194/acp-2020-501
Preprint. Discussion started: 21 July 2020


Atmospheric Chemistry and Physics Discussions

484 Dawson, M. L., V. Perraud, A. Gomez, K. D. Arquero, M. J. Ezell, and B. J. Finlayson-Pitts.
485 Measurement of gas-phase ammonia and amines in air by collection onto an ion exchange resin
486 and analysis by ion chromatography, Atmos. Meas. Tech., 7: 2733-44, 2014

487 Day, Derek, and William Malm. Aerosol light scattering measurements as a function of relative
488 humidity: A comparison between measurements made at three different sites, Atmospheric
489 Environment, 35: 5169-76, 2001

490 DeCarlo, P. F., E. J. Dunlea, J. R. Kimmel, A. C. Aiken, D. Sueper, J. Crounse, P. O. Wennberg,
491 L. Emmons, Y. Shinozuka, A. Clarke, J. Zhou, J. Tomlinson, D. R. Collins, D. Knapp, A. J.
492 Weinheimer, D. D. Montzka, T. Campos, and J. L. Jimenez. Fast airborne aerosol size and
493 chemistry measurements above Mexico City and Central Mexico during the MILAGRO campaign,
494 Atmos. Chem. Phys., 8: 4027-48, 2008

495 DeCarlo, Peter, Joel Kimmel, Achim Trimborn, Megan Northway, John Jayne, Allison Aiken,
496 Marc Gonin, Katrin Fuhrer, Thomas Horvath, Kenneth Docherty, Doug Worsnop, and Jose
497 Jimenez. Field-Deployable, High-Resolution, Time-of-Flight Aerosol Mass Spectrometer,
498 Analytical Chemistry, 78: 8281-9, 2007

499 Dibb, J. E., Talbot, R. W., Scheuer, E. M., Seid, G., Avery, M. A., and Singh, H. B.: Aerosol
500 chemical composition in Asian continental outflow during the TRACE-P campaign: Comparison
501 with PEM-West B, J. Geophys. Res., 108, 8815, https://doi.org/10.1029/2002JD003111, 2003

502 Ding, J., P. Zhao, J. Su, Q. Dong, X. Du, and Y. Zhang. Aerosol pH and its driving factors in
503 Beijing, Atmos. Chem. Phys., 19: 7939-54, 2019

504 Diskin, G. S., Podolske, J. R., Sachse, G. W. and Slate, T. A.: Open-path airborne tunable diode
505 laser hygrometer, in Diode Lasers and Applications in Atmospheric Sensing, vol. 4817, pp. 196–
506 204, International Society for Optics and Photonics., 2002

507 Drewnick, F., S. S. Hings, M. R. Alfarra, A. S. H. Prevot, and S. Borrmann. Aerosol quantification
508 with the Aerodyne Aerosol Mass Spectrometer: detection limits and ionizer background effects,
509 Atmos. Meas. Tech., 2: 33-46, 2009

510 Dunlea, E. J., P. F. DeCarlo, A. C. Aiken, J. R. Kimmel, R. E. Peltier, R. J. Weber, J. Tomlinson,
511 D. R. Collins, Y. Shinozuka, C. S. McNaughton, S. G. Howell, A. D. Clarke, L. K. Emmons, E.
512 C. Apel, G. G. Pfister, A. van Donkelaar, R. V. Martin, D. B. Millet, C. L. Heald, and J. L. Jimenez.

https://doi.org/10.5194/acp-2020-501
Preprint. Discussion started: 21 July 2020


Atmospheric Chemistry and Physics Discussions

513 Evolution of Asian aerosols during transpacific transport in INTEX-B, Atmos. Chem. Phys., 9:
514 7257-87, 2009

515 Duyzer, J. Dry deposition of ammonia and ammonium aerosols over heathland, Journal of
516 Geophysical Research: Atmospheres, 99: 18757-63, 1994

517 Fang, T., Guo, H. Zeng, L., Verma, V., Nenes, A., and Weber, R.J. Highly Acidic Ambient
518 Particles, Soluble Metals, and Oxidative Potential: A Link between Sulfate and Aerosol Toxicity,
519 Environmental Science & Technology, 51: 2611-20, 2017

520 Farmer, D. K., A. Matsunaga, K. S. Docherty, J. D. Surratt, J. H. Seinfeld, P. J. Ziemann, and J.
521 L. Jimenez. Response of an aerosol mass spectrometer to organonitrates and organosulfates and
522 implications for atmospheric chemistry, Proceedings of the National Academy of Sciences, 107:
523 6670-75, 2010

524 Fountoukis, C., and A. Nenes. ISORROPIA II: a computationally efficient thermodynamic
525 equilibrium model for K+ - Ca2+ - Mg2+ - NH4+ - Na+ - SO42- - NO3- - Cl- - H2O aerosols,
526 Atmos. Chem. Phys., 7: 4639-59, 2007

527 Fountoukis, C., A. Nenes, A. Sullivan, R. Weber, T. Van Reken, M. Fischer, E. Matías, M. Moya,
528 D. Farmer, and R. C. Cohen. Thermodynamic characterization of Mexico City aerosol during
529 MILAGRO 2006, Atmos. Chem. Phys., 9: 2141-56, 2009

530 Fry, J. L., Draper, D. C., Zarzana, K. J., Campuzano-Jost, P., Day, D. A., Jimenez, J. L., Brown,
531 S. S., Cohen, R. C., Kaser, L., Hansel, A., Cappellin, L., Karl, T., Hodzic Roux, A., Turnipseed,
532 A., Cantrell, C., Lefer, B. L. and Grossberg, N.: Observations of gas- and aerosol-phase organic
533 nitrates at BEACHON-RoMBAS 2011, Atmos. Chem. Phys., 13(17), 8585–8605,
534 doi:10.5194/acp-13-8585-2013, 2013

535 Ghio, Andrew J., Martha Sue Carraway, and Michael C. Madden. Composition of Air Pollution
536 Particles and Oxidative Stress in Cells, Tissues, and Living Systems, Journal of Toxicology and
537 Environmental Health, Part B, 15: 1-21, 2012

538 Guo, H., J. Liu, K. D. Froyd, J. M. Roberts, P. R. Veres, P. L. Hayes, J. L. Jimenez, A. Nenes, and
539 R. J. Weber. Fine particle pH and gas–particle phase partitioning of inorganic species in Pasadena,
540 California, during the 2010 CalNex campaign, Atmos. Chem. Phys., 17: 5703-19, 2017

https://doi.org/10.5194/acp-2020-501
Preprint. Discussion started: 21 July 2020

541 Guo, H., A. Nenes, and R. J. Weber. The underappreciated role of nonvolatile cations in aerosol
542 ammonium-sulfate molar ratios, Atmos. Chem. Phys., 18: 17307-23, 2018a

543 Guo, H., R. Otjes, P. Schlag, A. Kiendler-Scharr, A. Nenes, and R. J. Weber. Effectiveness of
544 ammonia reduction on control of fine particle nitrate, Atmos. Chem. Phys., 18: 12241-56, 2018b

545 Guo, H., L. Xu, A. Bougiatioti, K. M. Cerully, S. L. Capps, J. R. Hite Jr, A. G. Carlton, S. H. Lee,
546 M. H. Bergin, N. L. Ng, A. Nenes, and R. J. Weber. Fine-particle water and pH in the southeastern
547 United States, Atmos. Chem. Phys., 15: 5211-28, 2015

548 Guo, Hongyu, Amy P. Sullivan, Pedro Campuzano-Jost, Jason C. Schroder, Felipe D. Lopez-
549 Hilfiker, Jack E. Dibb, Jose L. Jimenez, Joel A. Thornton, Steven S. Brown, Athanasios Nenes,
550 and Rodney J. Weber. Fine particle pH and the partitioning of nitric acid during winter in the
551 northeastern United States, Journal of Geophysical Research: Atmospheres, 121: 10,355-10,76,
552 2016

553 Guo, Hongyu, Rodney J. Weber, and Athanasios Nenes. High levels of ammonia do not raise fine
554 particle pH sufficiently to yield nitrogen oxide-dominated sulfate production, Scientific Reports,
555 7: 12109, 2017

556 Gwynn, R. C., R. T. Burnett, and G. D. Thurston. A time-series analysis of acidic particulate matter
557 and daily mortality and morbidity in the Buffalo, New York, region, Environmental health
558 perspectives, 108: 125-33, 2000

559 Heim, E., J.E. Dibb, E. Scheuer, P. Campuzano-Jost, B.A. Nault, J.L. Jimenez, D. Peterson, C.
560 Knote, M. Fenn, J. Hair, A.J. Beyersdorf, C. Corr, B.E. Anderson. Asian Dust Observed during
561 KORUS-AQ Facilitates the Uptake and Incorporation of Soluble Pollutants during Transport to
562 South Korea. Atmos. Environ., in press, 2020

563 Hennigan, C. J., J. Izumi, A. P. Sullivan, R. J. Weber, and A. Nenes. A critical evaluation of proxy
564 methods used to estimate the acidity of atmospheric particles, Atmos. Chem. Phys., 15: 2775-90,
565 2015

566 Hong, Jong Ho, Jitae Kim, Wonik Son, Heeyoung Shin, Nahyun Kim, Woong Ki Lee, and Jintae
567 Kim. Long-term energy strategy scenarios for South Korea: Transition to a sustainable energy
568 system, Energy Policy, 127: 425-37, 2019

https://doi.org/10.5194/acp-2020-501
Preprint. Discussion started: 21 July 2020


Atmospheric Chemistry and Physics Discussions

569 Huebert, B. J., and C. H. Robert. The dry deposition of nitric acid to grass, Journal of Geophysical
570 Research: Atmospheres, 90: 2085-90, 1985

571 Huey, L. G., D. J. Tanner, D. L. Slusher, J. E. Dibb, R. Arimoto, G. Chen, D. Davis, M. P. Buhr,
572 J. B. Nowak, R. L. Mauldin, F. L. Eisele, and E. Kosciuch. CIMS measurements of HNO3 and
573 SO2 at the South Pole during ISCAT 2000, Atmospheric Environment, 38: 5411-21 2004

574 Huey, L. Gregory, Peter W. Villalta, Edward J. Dunlea, David R. Hanson, and Carleton J. Howard.
575 Reactions of CF3O- with Atmospheric Trace Gases, The Journal of Physical Chemistry, 100: 190-
576 94, 1996

577 Huffman, J. A., K. S. Docherty, A. C. Aiken, M. J. Cubison, I. M. Ulbrich, P. F. DeCarlo, D.
578 Sueper, J. T. Jayne, D. R. Worsnop, P. J. Ziemann, and J. L. Jimenez. Chemically-resolved aerosol
579 volatility measurements from two megacity field studies, Atmos. Chem. Phys., 9: 7161-82, 2009

580 Ito, T., Nenes, A., Johnson, M. S., Meskhidze, N., Valett, J., and Deutsch, C. Late 20th century
581 deoxygenation of the tropical Pacific enhanced by aerosol pollutants, Nature Geosci.,
582 doi:10.1038/ngeo2717, 2016

583 Jordan, Carolyn E. , James H. Crawford, Andreas J. Beyersdorf, Thomas F. Eck, Hannah S.
584 Halliday, Benjamin A. Nault, Lim-Seok Chang, Rokjin Park, Gangwoong Lee, Hwajin Kim,
585 Seogju Cho, Hye Jung Shin, Jae Hong Lee, Jinsang Jung, Deug-Soo Kim, Meehye Lee, Taehyoung
586 Lee, Andrew Whitehill, James Szykman, Melinda Kaye Schueneman, Pedro Campuzano Jost, Jose
587 L. Jimenez, Joshua P. DiGangi, Glenn S. Diskin, Bruce E. Anderson, Richard H. Moore, Luke D.
588 Ziemba, Marta A. Fenn, Johnathan W. Hair, Ralph E. Kuehn, Robert E. Holz, Gao Chen, Katherine
589 Travis, Michael Shook, David A. Peterson, Kara D. Lamb, Joshua P. Schwarz. Investigation of
590 Factors Controlling PM2.5 Variability across the South Korean peninsula during KORUS-AQ,
591 Elementa, in review

592 Kafle, Sagar, Ranjan Parajuli, Sujala Bhattarai, Seung Hee Euh, and Dae Hyun Kim. A review on
593 energy systems and GHG emissions reduction plan and policy of the Republic of Korea: Past,
594 present, and future, Renewable and Sustainable Energy Reviews, 73: 1123-30, 2017

595 Kim, Minjoong J. Sensitivity of Nitrate Aerosol Production to Vehicular Emissions in an Urban
596 Street, Atmosphere, 10: 212, 2019

https://doi.org/10.5194/acp-2020-501
Preprint. Discussion started: 21 July 2020


Atmospheric Chemistry and Physics Discussions

597 Kim, Na Kyung, Yong Pyo Kim, Yu Morino, Jun-ichi Kurokawa, and Toshimasa Ohara.
598 Verification of NOx emission inventory over South Korea using sectoral activity data and satellite
599 observation of NO2 vertical column densities, Atmospheric Environment, 77: 496-508, 2013

600 Kim, S., L. G. Huey, R. E. Stickel, D. J. Tanner, J. H. Crawford, J. R. Olson, G. Chen, W. H.
601 Brune, X. Ren, R. Lesher, P. J. Wooldridge, T. H. Bertram, A. Perring, R. C. Cohen, B. L. Lefer,
602 R. E. Shetter, M. Avery, G. Diskin, and I. Sokolik. Measurement of HO2NO2 in the free
603 troposphere during the Intercontinental Chemical Transport Experiment–North America 2004,
604 Journal of Geophysical Research: Atmospheres, 112, 2007

605 Kim, H., Zhang, Q., and Heo, J.: Influence of intense secondary aerosol formation and long-range
606 transport on aerosol chemistry and properties in the Seoul Metropolitan Area during spring time:
607 results from KORUS-AQ, Atmos. Chem. Phys., 18, 7149–7168, https://doi.org/10.5194/acp-18-
608 7149-2018, 2018

609 Kimmel, Joel R., Delphine K. Farmer, Michael J. Cubison, Donna Sueper, Christian Tanner, Eiko
610 Nemitz, Douglas R. Worsnop, Marc Gonin, and Jose L. Jimenez. Real-time aerosol mass
611 spectrometry with millisecond resolution, International Journal of Mass Spectrometry, 303: 15-26,
612 2011

613 Koutrakis, Petros, Jack M. Wolfson, and John D. Spengler. An improved method for measuring
614 aerosol strong acidity: Results from a nine-month study in St Louis, Missouri and Kingston,
615 Tennessee, Atmospheric Environment, 22: 157-62, 1987

616 Lelieveld, J., J. S. Evans, M. Fnais, D. Giannadaki, and A. Pozzer. The contribution of outdoor air
617 pollution sources to premature mortality on a global scale, Nature, 525: 367-71, 2015

618 Meskhidze, N., W. L. Chameides, A. Nenes, and G. Chen. Iron mobilization in mineral dust: Can
619 anthropogenic SO2 emissions affect ocean productivity?, Geophysical Research Letters, 30, 2003

620 Nakao, Motoyuki, Yoko Ishihara, Cheol-Hong Kim, and In-Gyu Hyun. The Impact of Air
621 Pollution, Including Asian Sand Dust, on Respiratory Symptoms and Health-related Quality of
622 Life in Outpatients With Chronic Respiratory Disease in Korea: A Panel Study, Journal of
623 preventive medicine and public health = Yebang Uihakhoe chi, 51: 130-39, 2018

624 Nault, B. A., P. Campuzano-Jost, D. A. Day, J. C. Schroder, B. Anderson, A. J. Beyersdorf, D. R.
625 Blake, W. H. Brune, Y. Choi, C. A. Corr, J. A. de Gouw, J. Dibb, J. P. DiGangi, G. S. Diskin, A.

https://doi.org/10.5194/acp-2020-501
Preprint. Discussion started: 21 July 2020


Atmospheric Chemistry and Physics Discussions

626 Fried, L. G. Huey, M. J. Kim, C. J. Knote, K. D. Lamb, T. Lee, T. Park, S. E. Pusede, E. Scheuer,
627 K. L. Thornhill, J. H. Woo, and J. L. Jimenez. Secondary organic aerosol production from local
628 emissions dominates the organic aerosol budget over Seoul, South Korea, during KORUS-AQ,
629 Atmos. Chem. Phys., 18: 17769-800, 2018

630 Nenes, A., M. D. Krom, N. Mihalopoulos, P. Van Cappellen, Z. Shi, A. Bougiatioti, P. Zarmpas,
631 and B. Herut. Atmospheric acidification of mineral aerosols: a source of bioavailable phosphorus
632 for the oceans, Atmos. Chem. Phys., 11: 6265-72, 2011

633 Nenes, A., Pandis, S. N., Weber, R. J., and Russell, A.: Aerosol pH and liquid water content
634 determine when particulate matter is sensitive to ammonia and nitrate availability, Atmos. Chem.
635 Phys., 20, 3249–3258, https://doi.org/10.5194/acp-20-3249-2020, 2020a

636 Nenes, A., Pandis, S. N., Kanakidou, M., Russell, A., Song, S., Vasilakos, P., Weber, R. J.: Aerosol
637 acidity and liquid water content regulate the dry deposition of inorganic reactive nitrogen, Atmos.
638 Chem. Phys. Disc., in review, 2020b

639 Osada, Kazuo. Measurements of Gaseous NH3 and Particulate NH4+ in the Atmosphere by
640 Fluorescent Detection after Continuous Air–water Droplet Sampling, Aerosol and Air Quality
641 Research, 2011

642 Pozzer, A., A. P. Tsimpidi, V. A. Karydis, A. de Meij, and J. Lelieveld. Impact of agricultural
643 emission reductions on fine-particulate matter and public health, Atmos. Chem. Phys., 17: 12813-
644 26, 2017

645 Pye, H. O. T., A. Nenes, B. Alexander, A. P. Ault, M. C. Barth, S. L. Clegg, J. L. Collett Jr, K. M.
646 Fahey, C. J. Hennigan, H. Herrmann, M. Kanakidou, J. T. Kelly, I. T. Ku, V. F. McNeill, N.
647 Riemer, T. Schaefer, G. Shi, A. Tilgner, J. T. Walker, T. Wang, R. Weber, J. Xing, R. A. Zaveri,
648 and A. Zuend. The Acidity of Atmospheric Particles and Clouds, Atmos. Chem. Phys., in press,
649 2020

650 Raizenne, M., L. M. Neas, A. I. Damokosh, D. W. Dockery, J. D. Spengler, P. Koutrakis, J. H.
651 Ware, and F. E. Speizer. Health effects of acid aerosols on North American children: pulmonary
652 function, Environmental health perspectives, 104: 506-14, 1996

653 Riemer, N., Ault, A. P., West, M.,Craig, R. L., & Curtis, J. H. Aerosol mixing state: Measurements,
654 modeling, and impacts, Reviews of Geophysics, 57, 187–249, 2019

655 RSSR: Introduction to the KORUS-AQ Rapid Science Synthesis Report.
656 https://espo.nasa.gov/sites/default/files/documents/KORUS-AQ-ENG.pdf, 2016

657 Saide, P. E., Gao, M., Lu, Z., Goldberg, D., Streets, D. G., Woo, J.-H., Beyersdorf, A., Corr, C.
658 A., Thornhill, K. L., Anderson, B., Hair, J. W., Nehrir, A. R., Diskin, G. S., Jimenez, J. L., Nault,
659 B. A., Campuzano-Jost, P., Dibb, J., Heim, E., Lamb, K. D., Schwarz, J. P., Perring, A. E., Kim,
660 J., Choi, M., Holben, B., Pfister, G., Hodzic, A., Carmichael, G. R., Emmons, L., and Crawford,
661 J. H. Understanding and improving model representation of aerosol optical properties for a Chinese
662 haze event measured during KORUS-AQ, Atmos. Chem. Phys. Discuss.,
663 https://doi.org/10.5194/acp-2019-1022, in review, 2019.

664 Schrader, F., and Brümmer., C. Land Use Specific Ammonia Deposition Velocities: a Review of
665 Recent Studies (2004-2013), Water, Air, and Soil Pollution, 225: 2114-14, 2014

666 Seinfeld, J.H. and Pandis, S.N. Atmospheric Chemistry and Physics: From Air Pollution to Climate
667 Change. John Wiley & Sons, Hoboken, 2016.

668 Shingler, T., Crosbie, E., Ortega, A., Shiraiwa, M., Zuend, A., Beyersdorf, A., Ziemba, L.,
669 Anderson, B., Thornhill, L., Perring, A. E., Schwarz, J. P., Campazano-Jost, P., Day, D. A.,
670 Jimenez, J. L., Hair, J. W., Mikoviny, T., Wisthaler, A. and Sorooshian, A.: Airborne
671 Characterization of Sub-saturated Aerosol Hygroscopicity and Dry Refractive Index from the
672 Surface to 6.5 km during the SEAC 4 RS Campaign, J. Geophys. Res. Atmos., 121(8), 4188–4210,
673 doi:10.1002/2015JD024498, 2016

674 Slusher, Darlene L., L. Gregory Huey, David J. Tanner, Frank M. Flocke, and James M. Roberts.
675 A thermal dissociation–chemical ionization mass spectrometry (TD-CIMS) technique for the
676 simultaneous measurement of peroxyacyl nitrates and dinitrogen pentoxide, Journal of
677 Geophysical Research: Atmospheres, 109, 2004

678 Song, S., M. Gao, W. Xu, J. Shao, G. Shi, S. Wang, Y. Wang, Y. Sun, and M. B. McElroy. Fine-
679 particle pH for Beijing winter haze as inferred from different thermodynamic equilibrium models,
680 Atmos. Chem. Phys., 18: 7423-38, 2018

681 Song, S., M. Gao, W. Xu, Y. Sun, D. R. Worsnop, J. T. Jayne, Y. Zhang, L. Zhu, M. Li, Z. Zhou,
682 C. Cheng, Y. Lv, Y. Wang, W. Peng, X. Xu, N. Lin, Y. Wang, S. Wang, J. W. Munger, D. J. Jacob,

https://doi.org/10.5194/acp-2020-501
Preprint. Discussion started: 21 July 2020


Atmospheric Chemistry and Physics Discussions

683 and M. B. McElroy. Possible heterogeneous chemistry of hydroxymethanesulfonate (HMS) in
684 northern China winter haze, Atmos. Chem. Phys., 19: 1357-71, 2019

685 Tan, Tianyi, Min Hu, Mengren Li, Qingfeng Guo, Yusheng Wu, Xin Fang, Fangting Gu, Yu
686 Wang, and Zhijun Wu. New insight into PM2.5 pollution patterns in Beijing based on one-year
687 measurement of chemical compositions, Science of The Total Environment, 621: 734-43, 2018

688 Thurston, G. D., K. Ito, C. G. Hayes, D. V. Bates, and M. Lippmann. Respiratory Hospital
689 Admissions and Summertime Haze Air Pollution in Toronto, Ontario: Consideration of the Role
690 of Acid Aerosols, Environmental Research, 65: 271-90, 1994

691 Vasilakos, P., A. Russell, R. Weber, and A. Nenes. Understanding nitrate formation in a world
692 with less sulfate, Atmos. Chem. Phys., 18: 12765-75, 2018

693 Wang, Haiting, Jing Ding, Jiao Xu, Jie Wen, Jianhong Han, Keling Wang, Guoliang Shi, Yinchang
694 Feng, Cesunica E. Ivey, Yuhang Wang, Athanasios Nenes, Qianyu Zhao, and Armistead G.
695 Russell. Aerosols in an arid environment: The role of aerosol water content, particulate acidity,
696 precursors, and relative humidity on secondary inorganic aerosols, Science of The Total
697 Environment, 646: 564-72, 2019

698 Wang, Shanshan, Jialiang Nan, Chanzhen Shi, Qingyan Fu, Song Gao, Dongfang Wang, Huxiong
699 Cui, Alfonso Saiz-Lopez, and Bin Zhou. Atmospheric ammonia and its impacts on regional air
700 quality over the megacity of Shanghai, China, Scientific Reports, 5: 15842, 2015

701 Warner, J. X., R. R. Dickerson, Z. Wei, L. L. Strow, Y. Wang, and Q. Liang. Increased atmospheric
702 ammonia over the world's major agricultural areas detected from space, Geophysical Research
703 Letters, 44: 2875-84., 2017

704 Womack, C. C., E. E. McDuffie, P. M. Edwards, R. Bares, J. A. de Gouw, K. S. Docherty, W. P.
705 Dubé, D. L. Fibiger, A. Franchin, J. B. Gilman, L. Goldberger, B. H. Lee, J. C. Lin, R. Long, A.
706 M. Middlebrook, D. B. Millet, A. Moravek, J. G. Murphy, P. K. Quinn, T. P. Riedel, J. M. Roberts,
707 J. A. Thornton, L. C. Valin, P. R. Veres, A. R. Whitehill, R. J. Wild, C. Warneke, B. Yuan, M.
708 Baasandorj, and S. S. Brown. An Odd Oxygen Framework for Wintertime Ammonium Nitrate
709 Aerosol Pollution in Urban Areas: NOx and VOC Control as Mitigation Strategies, Geophysical
710 Research Letters, 46: 4971-79, 2019

https://doi.org/10.5194/acp-2020-501
Preprint. Discussion started: 21 July 2020

711 Xu, Z., M. Liu, Y. Song, S. Wang, L. Zhang, T. Xu, T. Wang, C. Yan, T. Zhou, Y. Sun, Y. Pan,
712 m. Hu, M. Zheng, and T. Zhu, High efficiency of livestock ammonia emission controls on
713 alleviating particulate nitrate during a severe winter haze episode in northern China, Atm. Chem.
714 Phys., 19, 5605-5613, 2019

715 Yokelson, R. J., T. J. Christian, I. T. Bertschi, and W. M. Hao. Evaluation of adsorption effects on
716 measurements of ammonia, acetic acid, and methanol, Journal of Geophysical Research:
717 Atmospheres, 108, 2003

718 Zhu, L., D. K. Henze, J. O. Bash, K. E. C.-P., M. W. Shephard, M. Luo, and S. L. Capps. Sources
719 and Impacts of Atmospheric NH_3: Current Understanding and Frontiers for Modeling,
720 Measurements, and Remote Sensing in North America, Current Pollution Reports, 1: 95-116, 2015

721 Zhu, S., Sartelet, K.N., Zhang, Y., Nenes, A. Three-dimensional modelling of the mixing state of
722 particles over Greater Paris, J. Geoph.Res., 121, doi:10.1002/2015JD024241, 2016

723

https://doi.org/10.5194/acp-2020-501
Preprint. Discussion started: 21 July 2020

Atmospheric Chemistry and Physics Discussions

724 **Table 1:** Summary of selected KORUS and other campaign data.

Campaign	KORUS-AQ	Institute of Urban Meteorology	SEARCH	CalNex	SOAS	SENEX
Type of Measurement	Air	Ground	Ground	Ground	Air	Air
Year	2016	2017	2010	2013	2013	2013
Season	Summer	Spring, Summer, Fall, Winter	Late Summer Early Fall	Summer	Summer	Summer
Location	South Korea	Beijing, China	SE U.S.	SW U.S.	SE U.S.	SE U.S.
Average RH (%)	62±12	-	69±18	79±17	74±16	72±9
Avg. HNO_3 (μg m^{-3})	4.61±2.72	-	0.50±0.26	6.65 ± 7.03	0.36 ± 0.14	1.35 ± 0.66
Avg. NO_3 concentration (μg m^{-3})	8.09± 6.16	12.6 ± 14.2 (spring), 13.7 ± 21.0 (winter), 9.5 ± 9.5 (summer), 18.5 ± 19.5 (fall)	0.2±0.1	PM1: 3.58 ± 3.65	0.08 ± 0.08	0.28 ± 0.09
Average ε(NO_3)	58±24%	-	26±15%	39±16%	22±16%	18 ± 6 %
pH	2.43 ±0.68 (no NVCs) 2.45±0.96 (with NVCs)	4.3±1.6 (spring), 4.5±1.1 (winter), 3.9±1.3 (summer), 4.1±1.0 (fall)	2.2 ±0.6	1.9 ±0.5	0.9 ± 0.6	1.1 ± 0.4
Reference	This study	Ding et al. (2019)	Nah et al. (2018)	Guo et al. (2017)	Guo et al. (2015)	Xu et al. (2016)

725

https://doi.org/10.5194/acp-2020-501
Preprint. Discussion started: 21 July 2020


Atmospheric Chemistry and Physics Discussions

Figure Captions

Figure 1: Average inorganic PM_1 mass composition throughout the entire study and for altitudes below 1km. Average total mass is 22 μg m^{-3}.

Figure 2: Guo et al. (2016) method for constraining aerosol pH in the absence of NH_3 data.

Figure 3: Total ammonia (blue) and pH (red) as a function of iteration number using the Guo et al. (2016) algorithm.

Figure 4: The nitrate partitioning constrained pH (NPC-pH) method to obtain aerosol pH from nitrate partitioning observations.

Figure 5: Comparison of equilibrium nitrate partitioning retrieved from synthetic data vs. the value from the NPC-pH method. Meteorological conditions in the synthetic dataset cover a RH of 45-95%, Temperature 298K and SO_4, NO_3^T, NH_4^T of 0.1-10 μg m^{-3}, 0.2-110 μg m^{-3}, and 0.2-110 μg m^{-3}, respectively. Non-volatile cation concentrations were set to zero, and Cl- concentration was kept constant at 0.5 μg m^{-3}.

Figure 6: Particle phase fraction of total nitrate, $\varepsilon(NO_3^-)$ (blue curve) and total ammonium, $\varepsilon(NH_4^+)$ (red curve) versus pH for a temperature of 288 K and an aerosol liquid water content of 10 μg m^{-3}. The pink zone is a region where PM is sensitive to both HNO_3 and NH_3. Following the approach of Nenes et al. (2020a), the dotted black line represents a pre-defined threshold, below which the aerosol is deemed insensitive to changes in NH_3 and/or HNO_3.

Figure 7: (a) Flight trajectories for altitudes below 1km during KORUS-AQ, color mapped by NO_3^- levels. Highest concentrations of NO_3^- observed near Seoul, for which NO_x emissions are dominated by the transportation and energy industries. (b) NO_x emission sources in Korea labelled by industry.

Figure 8: Chemical domains for entire KORUS-AQ study data. Larger fraction of data falls in HNO_3 sensitive region as a result of moderate-high values of nitrate partitioning.

Figure 9: Chemical domains for (a) flight 15 and (b) flight 19. For Flight 15, a significant number of its data points are characterized by low nitrate partitioning values (approx. 30%)**. Flight 19 is characterized by high levels of particle nitrate, and moderate to high levels of nitrate partitioning. For these reasons, PM would be for response to NH_3 and HNO_3 for flights 15 and 19 respectively.

Figure 10: Chemical domains for entire KORUS-AQ study data, with symbols colored by the value of PM.

https://doi.org/10.5194/acp-2020-501
Preprint. Discussion started: 21 July 2020

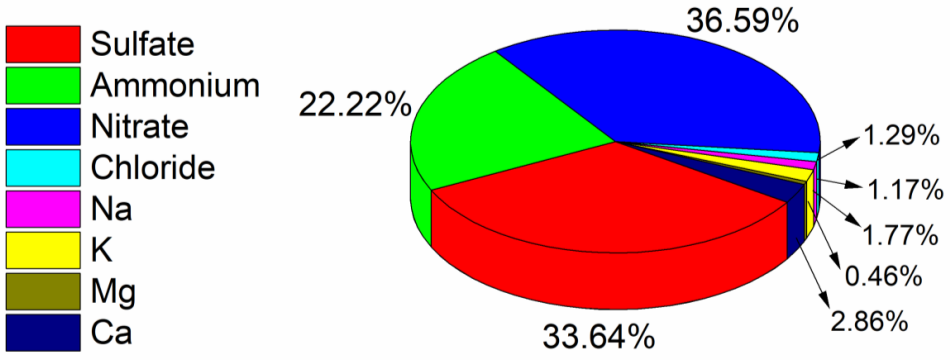

Figure 1

https://doi.org/10.5194/acp-2020-501
Preprint. Discussion started: 21 July 2020

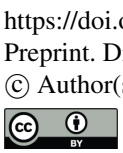

Atmospheric Chemistry and Physics Discussions

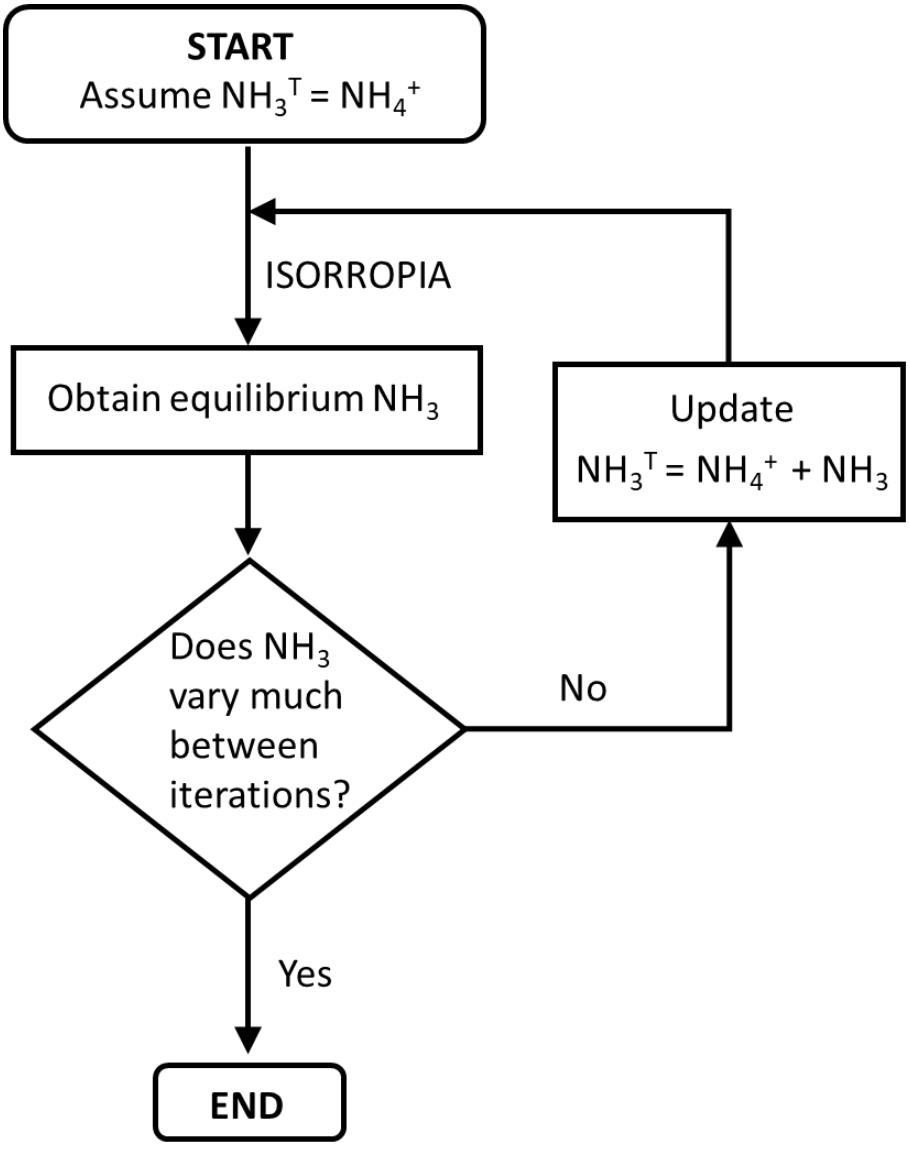

761
762 **Figure 2**
763

https://doi.org/10.5194/acp-2020-501
Preprint. Discussion started: 21 July 2020

Atmospheric Chemistry and Physics Discussions

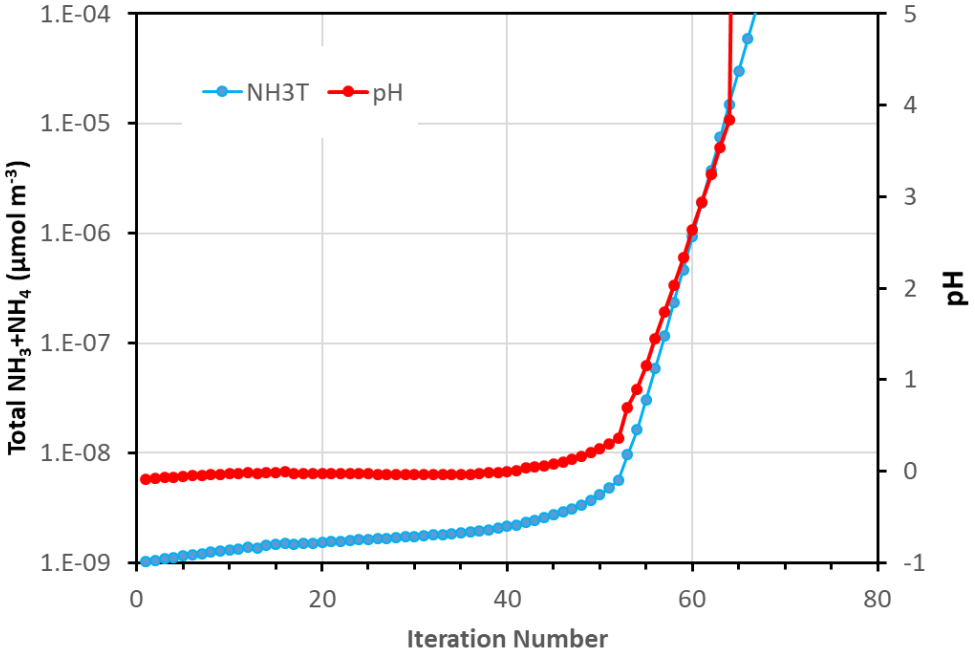

Figure 3

https://doi.org/10.5194/acp-2020-501
Preprint. Discussion started: 21 July 2020

Atmospheric Chemistry and Physics Discussions

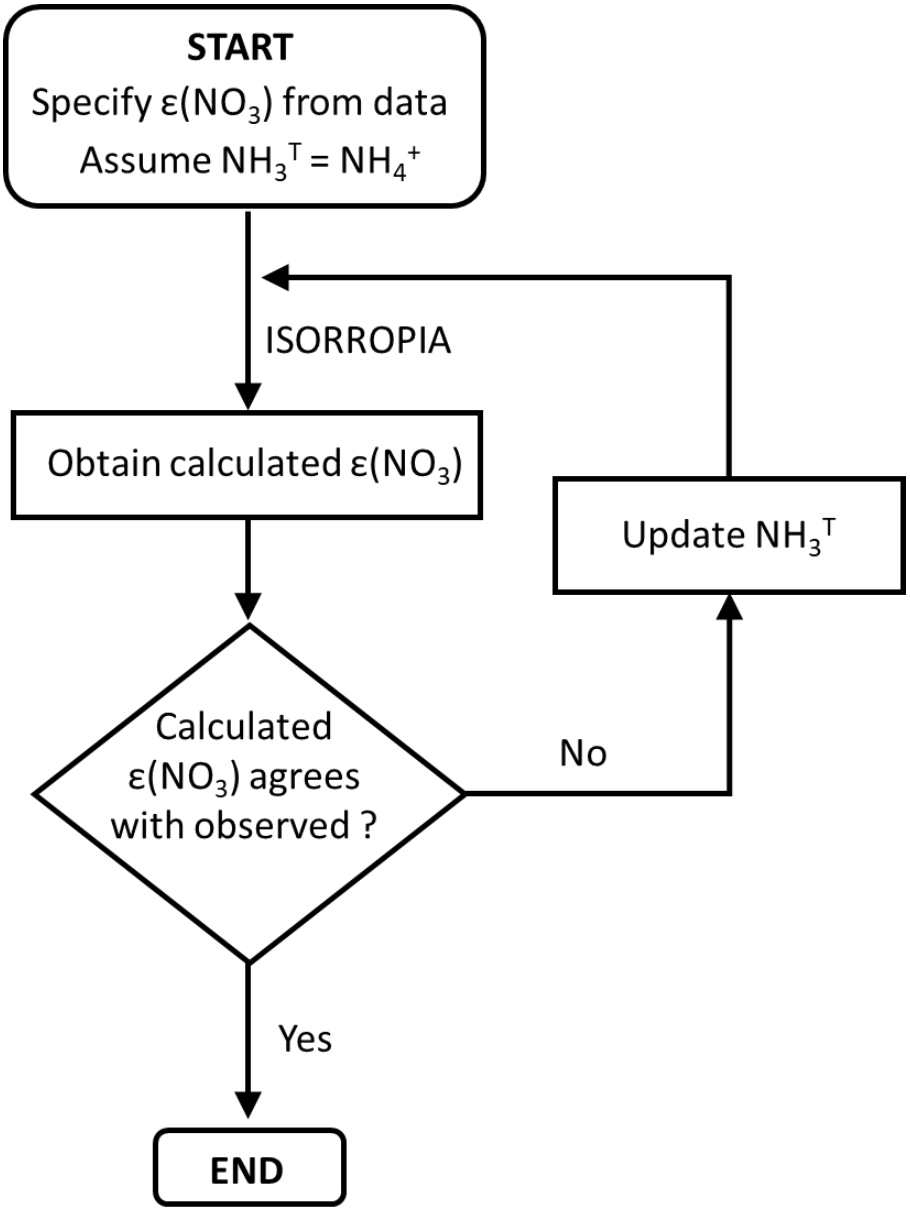

767
768
769 **Figure 4**
770

https://doi.org/10.5194/acp-2020-501
Preprint. Discussion started: 21 July 2020

Atmospheric Chemistry and Physics Discussions

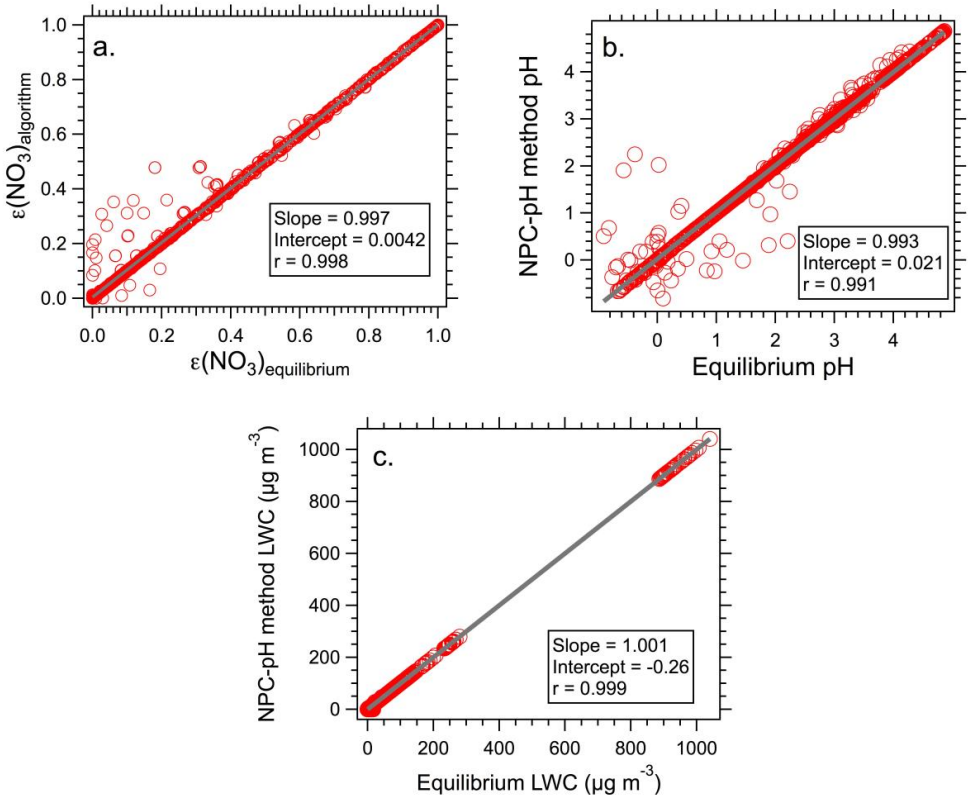

771
772
773 **Figure 5**
774

https://doi.org/10.5194/acp-2020-501
Preprint. Discussion started: 21 July 2020

Atmospheric Chemistry and Physics Discussions

775

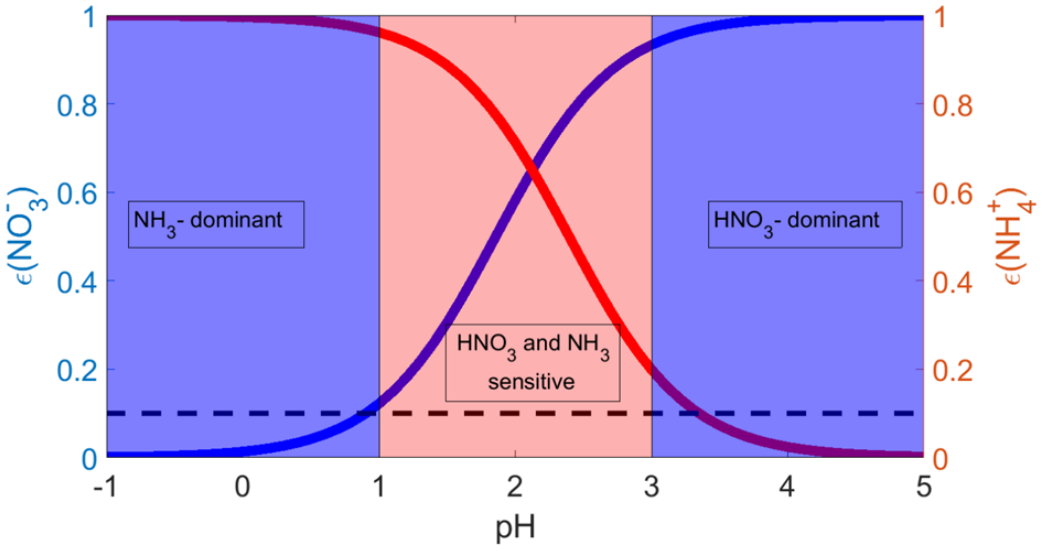

776
777 **Figure 6**
778

https://doi.org/10.5194/acp-2020-501
Preprint. Discussion started: 21 July 2020

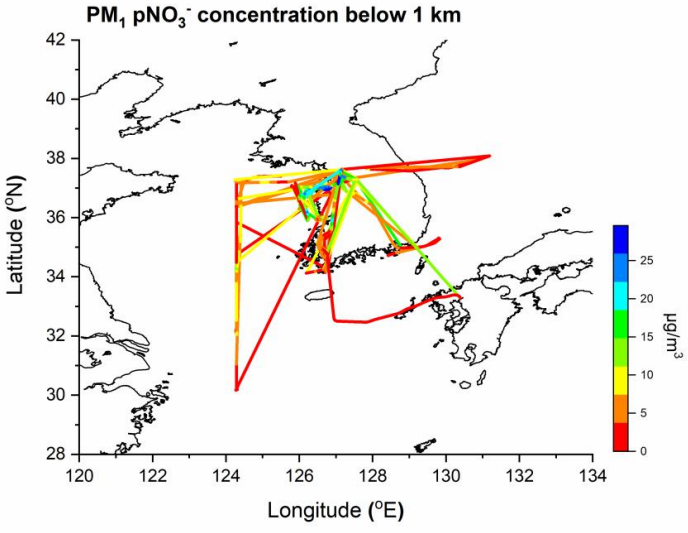

(a)

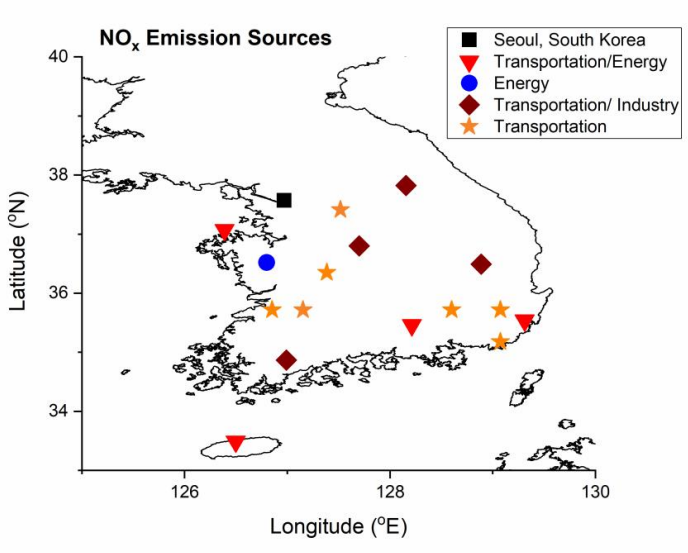

(b)

Figure 7

https://doi.org/10.5194/acp-2020-501
Preprint. Discussion started: 21 July 2020

Atmospheric Chemistry and Physics Discussions

787

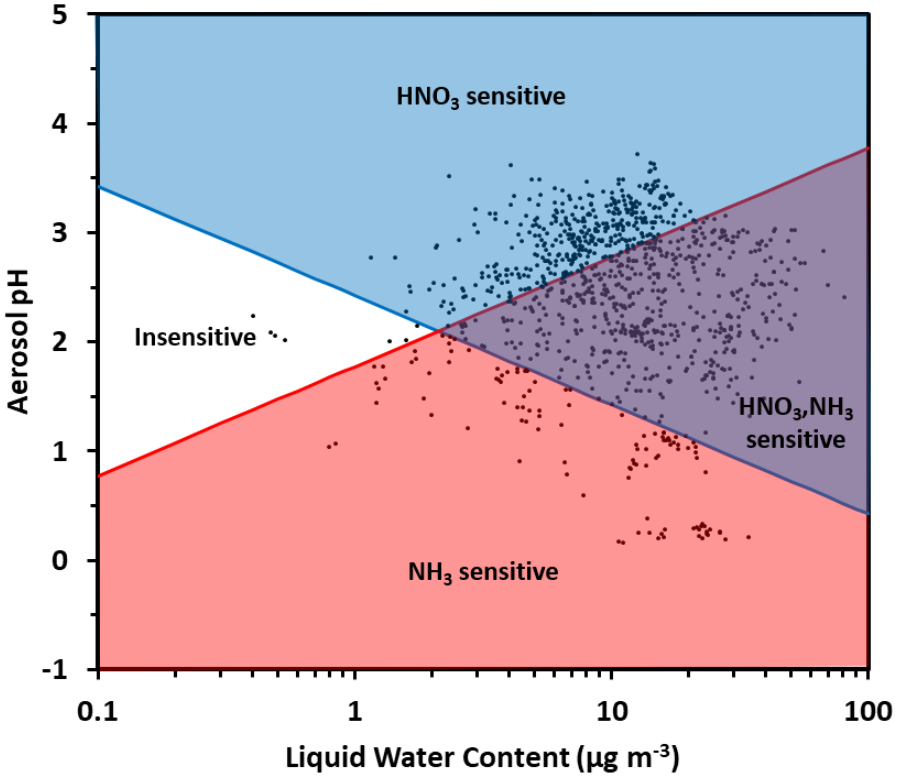

788
789 **Figure 8**
790
791
792
793

https://doi.org/10.5194/acp-2020-501
Preprint. Discussion started: 21 July 2020

Atmospheric Chemistry and Physics Discussions

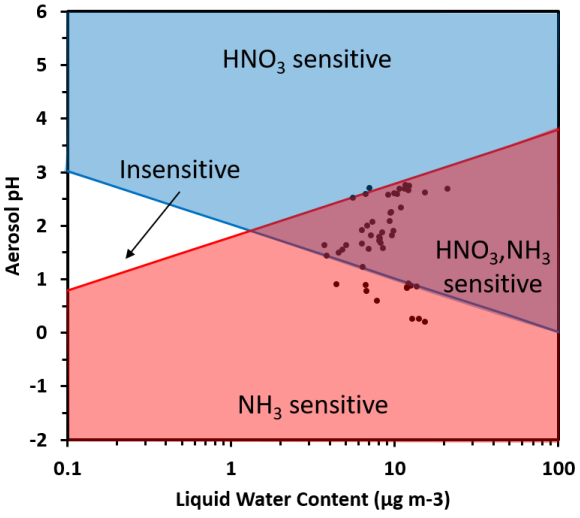

(a)

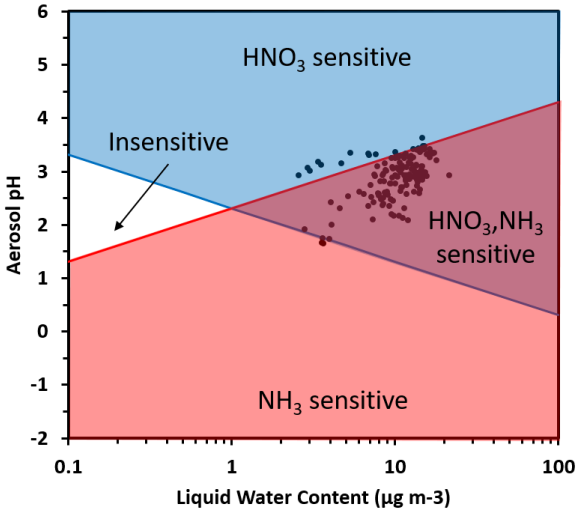

(b)

Figure 9

https://doi.org/10.5194/acp-2020-501
Preprint. Discussion started: 21 July 2020

Atmospheric Chemistry and Physics Discussions

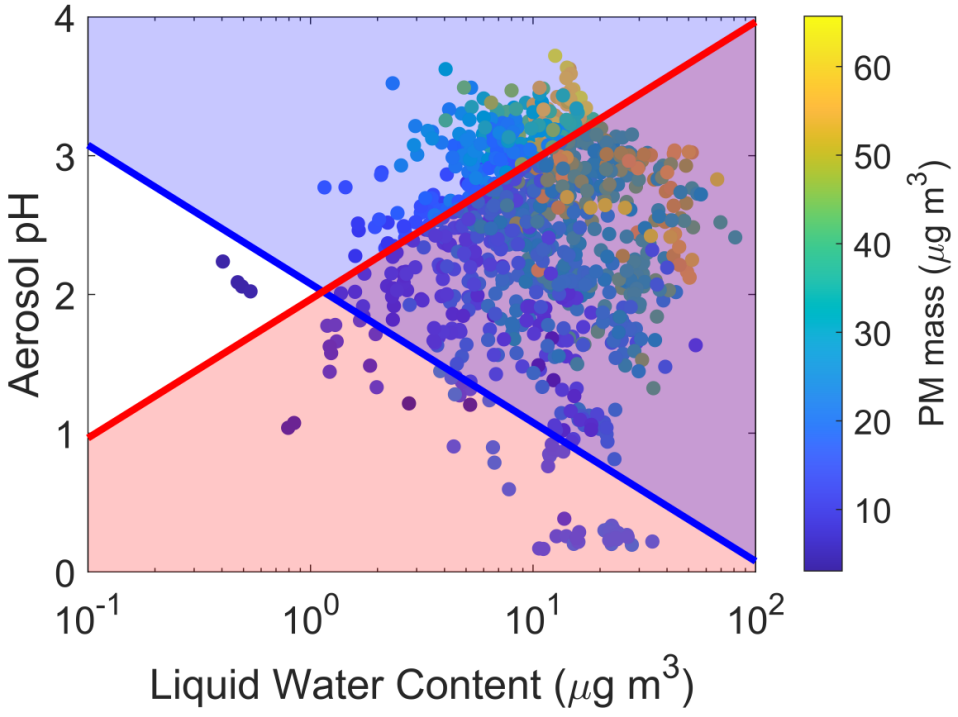

Figure 10